1981

# Proton transfers in hydrogen-bonded systems. VI. Electronic redistributions in (N2H7)+ and (O2H5)+

Steve Scheiner
*Utah State University*

# Proton transfers in hydrogen-bonded systems. VI. Electronic redistributions in $(N_2H_7)^+$ and $(O_2H_5)^{+a)}$

Steve Scheiner

*Department of Chemistry & Biochemistry, Southern Illinois University, Carbondale, Illinois 62901*

Electronic rearrangements accompanying transfer of the central proton between the two $XH_n$ units of $(H_3NHNH_3)^+$ and $(H_2OHOH_2)^+$ are studied using *ab initio* molecular orbital methods. Electron density difference maps are calculated by subtracting the density of the equilibrium structure (X–H---X) from that of the midpoint geometry (X--H--X) using the split-valence 4-31G basis set. Some of the features revealed by the maps are common to both systems while others indicate significant differences between nitrogen and oxygen. Decomposition of the total electron density into contributions from individual occupied molecular orbitals (MOs) provides insight into the factors responsible for the overall charge migrations. The orbitals of $a_1$ symmetry lead to density shifts in a direction parallel to the H bond axis. Among the features attributed to these MOs are the charge transfer across the H bond from one molecule to the other and characteristic density changes in the lone pair regions of the first-row X atoms. Internal polarizations of the XH bonds of each molecule arise from the density shifts perpendicular to the H bond axis associated with the MOs of non-$a_1$ symmetry. Simple arguments involving electrostatic and covalent effects are used to explain the redistributions observed in the various MOs. Mulliken analyses provide information, complementary to the difference maps, concerning the relative involvement of various atoms and atomic orbitals in the electronic redistributions associated with each MO.

## I. INTRODUCTION

Proton transfers are an integral part of a vast array of more complicated chemical and biological phenomena. Examples include such diverse processes as nucleophilic addition reactions, acid-base equilibria, enzyme catalysis, and photosynthesis.[1-6] Our greater understanding of these processes awaits a more detailed knowledge of each of the component steps including proton transfers. Determination of the energetics of transfer between various chemical groups would be of great importance. It would be valuable as well to have at hand some information concerning the effects of different intermolecular orientations upon the energetics. Of more fundamental interest is a description of the changes in electronic structure that are a direct result of the transfer of the proton.

These problems may be addressed very fruitfully by *ab initio* molecular orbital methods. Geometries may be specified with great precision and the energies of suitably chosen small model systems may be calculated with confidence in the reliability of the results. In addition, analyses of the wave functions lead to very detailed pictures of the electronic distributions at any stage of proton transfer.

A number of theoretical studies of proton transfer reactions have been carried out previously.[7-17] However, these investigations have for the most part concerned themselves with a single geometry of a particular system. In addition, little attempt has been made to identify the fundamental factors leading to the calculated energetics or to study the changes in electronic structure associated with the proton transfer. Recent work carried out in this laboratory[1-6] represents an attempt to provide systematic information about proton transfers in various systems and the effects on the transfer of distortions of the hydrogen bond.

In Paper IV of this series,[5] the energetics of proton transfer along the hydrogen bond were reported for the systems $(H_3NHNH_3)^+$ and $(H_2OHOH_2)^+$. The effects of stretches and bends of the hydrogen bond upon the energy barrier to the transfer were studied in some detail. It was demonstrated that for equivalent geometrical configurations, the barrier is uniformly higher for the $(O_2H_5)^+$ system than for $(N_2H_7)^+$. The rearrangements of the total electron density that accompany the proton transfer were also described for the first time in Paper IV. The two systems were shown to have certain features in common but several interesting differences were noted as well.

In an effort to study the fundamentals of the proton transfer process more intensively, the present paper describes a detailed analysis of the electronic redistributions. The total electron density of each system is decomposed here into contributions from each of the occupied molecular orbitals (MOs). The density shifts occurring within each MO provide a great deal of insight into the causes of the observed electronic structural changes. This analysis furnishes a useful framework by which to explain in a simple manner the general features of density shifts involved in the proton transfer process as well as the particular differences between the $(N_2H_7)^+$ and $(O_2H_5)^+$ systems.

## II. CALCULATIONS

The wave functions for the $(N_2H_7)^+$ and $(O_2H_5)^+$ systems were obtained using the Gaussian-70 system of programs.[18] The *ab initio* calculations were carried out at the Restricted Hartree-Fock level using the split valence-shell 4-31G basis set.[19] This basis set was chosen because it has been shown to yield results for these two systems in excellent agreement with much more sophisticated treatments using larger basis sets including polarization functions as well as treating electron correlation effects.[1-5] In addition, the splitting of the valence shell is expected to provide the flexibility required for
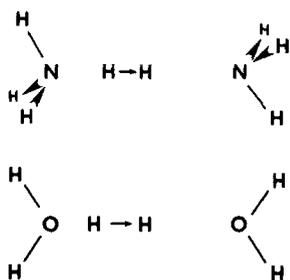
---

FIG. 1. Geometries of $(N_2H_7)^+$ and $(O_2H_5)^+$. All HNH angles are tetrahedral. The $r$(NH) bondlengths are 1.009 Å and 1.004 Å in the left- and right-hand $NH_3$ units, respectively. In the $H_2O$ units of $(O_2H_5)^+$, the $r$(OH) bondlengths are 0.95 Å and $\theta$(HOH) = 115°. Each arrow connects the equilibrium and midpoint positions of the central H.

proper description of the electronic distributions. The electron densities were calculated and plotted and the Mulliken population analyses[20] carried out using computer codes written in this laboratory.

The geometries of the $(N_2H_7)^+$ and $(O_2H_5)^+$ systems are illustrated in Fig. 1. As described in Paper IV, the fully optimized geometry of $(N_2H_7)^+$ was used as a starting point for the proton transfer. This structure contains a linear NH—N hydrogen bond with an internuclear R(NN) distance of 2.73 Å. The complex belongs to the $C_{3v}$ point group and the two $NH_3$ units are staggered with respect to one another. The hydrogen bond is asymmetric with the two r(NH) distances equal to 1.09 Å and 1.64 Å. We designate this structure as N–H---N; the left nitrogen is the proton donor and the other N is the acceptor.

Motion of the central H along the H-bond and towards the acceptor results in an increase in the total energy. Once the proton has reached the midpoint of the bond (N—H—N), further motion lowers the energy. The full potential for proton transfer is a symmetric double-well function with an energy barrier between the left and right-hand wells. This barrier is equal to the difference in energy between the peak of the potential function (N—H—N) and the equilibrium structure at the bottom of the well (N–H---N).

Because of the importance of the magnitude of the energy barrier to the kinetics of the transfer process, we concern ourselves here with the electronic rearrangements in the complex precipitated by motion of the proton from its equilibrium position near the donor molecule to the midpoint of the hydrogen bond. This half-transfer is illustrated schematically in Fig. 1 by the arrow connecting these two positions of the central proton. All atoms, with the exception of the central proton, are held stationary during the proton transfer. Previous calculations[1–5] have demonstrated that only very small changes are produced in the geometry or energetics by full geometry optimizations at each stage of proton transfer.

The arrow has an equivalent meaning in the $(O_2H_5)^+$ system. This complex is of $C_{2v}$ symmetry and all the atoms lie in the $yz$ plane. The R(OO) distance is set equal to 2.75 Å. (The equilibrium value of R(OO) is

2.36 Å[1], but this distance has been set equal to 2.75 Å here in order to facilitate comparison with the $(N_2H_7)^+$ system). For this interoxygen distance, the proton transfer potential is a symmetric double-well function. In the equilibrium structure at the bottom of the well O—H---O, the distances between the two oxygens and the central proton are 1.03 and 1.72 Å.

## III. TOTAL DENSITY REDISTRIBUTIONS

Shifts in total electron density resulting from half proton transfer are presented as contour maps in Fig. 2. Redistributions within the $xz$ plane of $(N_2H_7)^+$ are illustrated in Fig. 2(a). The atoms contained in this plane, including the two nitrogens and one H from each $NH_3$ unit, are represented by dots in the figure. The positions of the other hydrogens, located symmetrically above and below the $xz$ plane, are indicated by the heavy NH bond lines. While the $yz$ and $xz$ planes are equivalent for the $C_{3v}$ $(N_2H_7)^+$ system, the same is not true for $(O_2H_5)^+$ which belongs to the $C_{2v}$ point group. Therefore, electronic redistributions in both of these perpendicular planes are illustrated for $(O_2H_5)^+$ in Fig. 2(b). The oxygen nuclei and the two hydrogens located in the upper half of the $yz$ plane are indicated by dots. It should be pointed out that the $C_{2v}$ symmetry mandates that the density changes in the "hidden" portions of each plane are mirror images of those occurring in the half-planes shown.

As in Fig. 1, the tail of each arrow in Figs. 2(a) and 2(b) designates the equilibrium position of the central proton (X–H---X), and the arrowhead, its location at the midpoint of the hydrogen bond (X—H—X). The total electron density of each configuration was computed and the *difference* $[\rho(X—H—X) - \rho(X–H---X)]$ at each point in space is represented by the contours in Fig. 2. These maps thus illustrate the *shifts* in total electron density that accompany the motion of the central proton. Solid contours represent increases in density resulting from half proton transfer and decreases are denoted by broken contours. It should be noted that the numbers labeling each contour are proportional to the negative logarithm of the density changes occurring within the contour; hence, smaller numbers are associated with *larger* density differences.

It is important to distinguish the maps presented here from previously reported density difference maps[11,21–25] of hydrogen-bonded systems. The latter maps describe electronic structural changes resulting from formation of the complex $H_nAH$—$BH_m$ from two isolated reactants $H_nAH$ and $BH_m$ (H-bond formation) rather than the proton transfer within the H-bond under investigation here.

A number of features are common to both Figs. 2(a) and 2(b). The largest density changes are found to occur near the center of each H-bond. Density decrease (dashed contours) near the tail of each arrow and charge gain (solid curves) near the arrowhead demonstrate that, as expected, the transferring proton pulls substantial electron density along with it. Dashed contours to the left of each right-hand X nucleus indicate density loss in the region of the lone pair of the proton-accepting
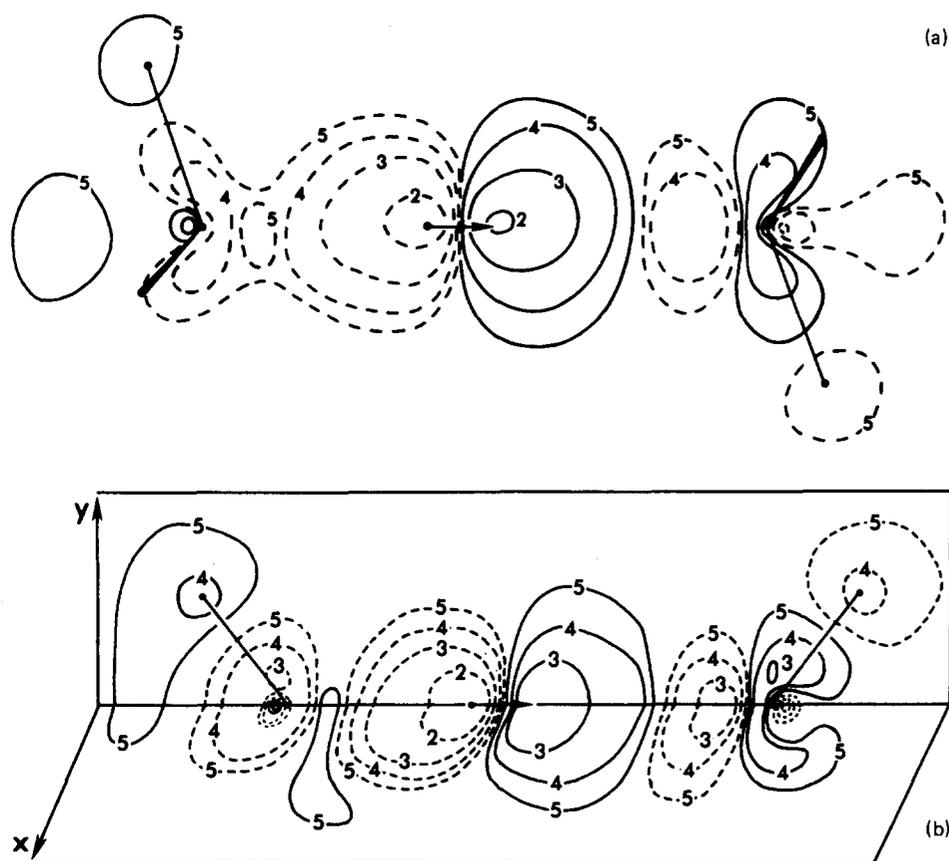
FIG. 2. Total electron density difference maps of (a) $(N_2H_7)^+$ and (b) $(O_2H_5)^+$ that accompany half transfer of the central proton (designated by the arrow). The density change occurring within each contour labeled "$n$" is equal to $10^{-n/2}$ e/a.u.[3] Solid and dashed contours respectively indicate gain and loss of density.

atom. Charge loss is noted also on the "outside", i.e., to the right, of the same atoms. The noncentral or "peripheral" H atoms of the proton-accepting molecules are located in regions of charge depletion, while the reverse is true of H atoms of each proton-donating molecule.

Besides basic similarities in Figs. 2(a) and 2(b), we note some significant and interesting differences. Whereas the lone pair region to the right of the proton-donating O atom shows some gain of electron density, there is no such increase in the corresponding area of the N atom. The "tail" regions of charge loss to the right of the proton-accepting N and O atoms are quite different in appearance. The same is true of the solid contours near these nuclei, and the dashed contours surrounding the proton-donating atoms.

Other differences include the magnitudes of density changes indicated by the appropriate contour labels. For example, in the lone pair region of the proton-accepting N atom, the smallest contour label is "4", whereas a "3" contour appears in the corresponding region of the O atom. This fact signifies a greater charge depletion in the lone pair of O than for the N atom. Similarly, the "4" labels surrounding the noncentral H atoms of the $(O_2H_5)^+$ complex, as compared to "5" contours for $(N_2H_7)^+$, indicate greater density changes for the H atoms in the former system.

## IV. ORBITAL REDISTRIBUTIONS

In order to provide some insights into the somewhat complex features of Fig. 2, the total electron density was partitioned into contributions from each of the doubly occupied molecular orbitals. The isoelectronic $(N_2H_7)^+$ and $(O_2H_5)^+$ systems each contain ten doubly occupied MO's. The orbitals of lowest energy $1a_1$ and $2a_1$ are comprised of the inner-shell $1s$ orbitals of the first-row X atoms. These nonvalence orbitals do not participate appreciably in electronic redistributions and are hence excluded from further consideration. The remaining eight occupied MOs of each of the two systems are illustrated schematically in Fig. 3. These MOs may be conveniently described as occurring in pairs as follows. The $3a_1$ and $4a_1$ orbitals consist primarily of bonding combinations of the $2s$ atomic orbital of each X atom with its neighboring H atoms. The lower energy orbital of the pair, $3a_1$, is a symmetric combination of the left- and right-hand molecules and contains also a small contribution from the $1s$ orbital of the central H. The $4a_1$ orbital is an antisymmetric combination and, as such, a nodal surface cuts perpendicularly across the midpoint of the X—X axis. The $(3a_1, 4a_1)$ pair may be considered chiefly as internal XH bonding orbitals.

The $(5a_1, 6a_1)$ pair of MOs contain principally X lone pair and hydrogen-bonding character. The lower energy $5a_1$ MO consists basically of a symmetric combination of the $Xp_z$ atomic orbitals and the $1s$ of the central H. $5a_1$ has a great deal of density focused near the center of the X—H—X bond and may be referred to as the "bridging" or "hydrogen bonding" MO. The $6a_1$ MO contains some mixing of the $2s$ with $2p_z$ atomic orbitals of each X to form hybrids pointing towards the center of the H-bond. The two hybrids are combined antisymmetrical-
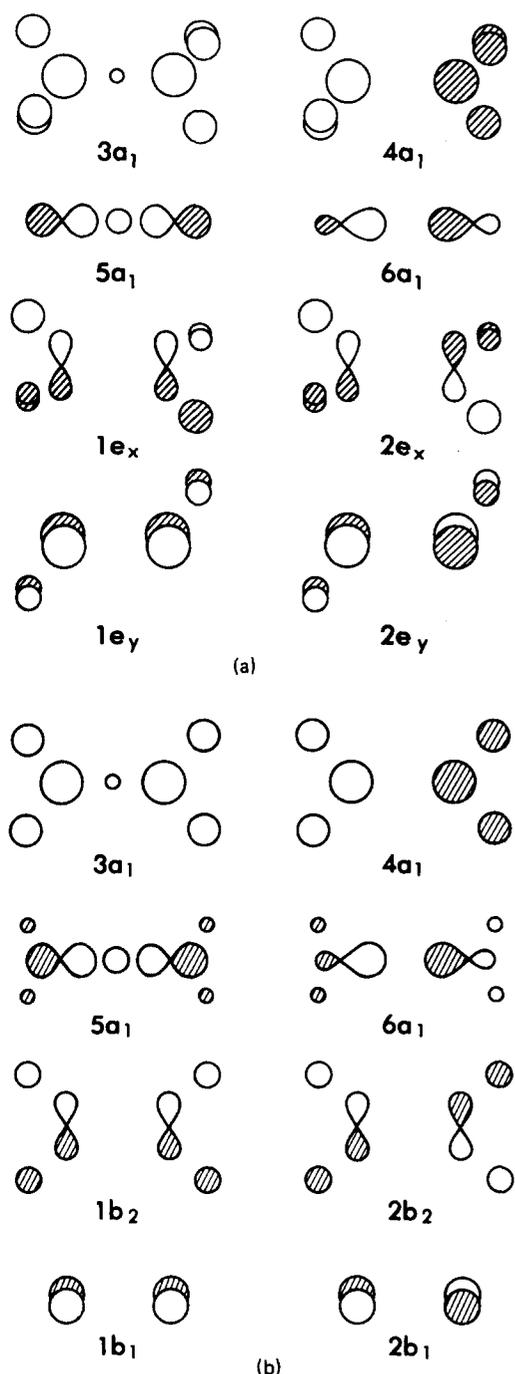
FIG. 3. Occupied MOs of (a) $(N_2H_7)^+$ and (b) $(O_2H_5)^+$. Cross-hatching represents negative sign of the wave function. Orbitals shown are for the X–H–X midpoint configuration and contain appropriate left–right symmetry.

ly with a nodal surface intersecting the bond at its center as shown in Fig. 3. The $(5a_1, 6a_1)$ pair of $(O_2H_5)^+$ also contain an appreciable contribution from the noncentral hydrogens. )

The remaining four occupied MOs of $(N_2H_7)^+$ are contained in two doubly degenerate levels $1e$ and $2e$. One MO of each level $(e_x)$ has a node in the $yz$ plane and the other $(e_y)$ in the $xz$ plane. The two $e$ pairs may thus be further categorized as $(1e_x, 2e_x)$ and $(1e_y, 2e_y)$. These two pairs are equivalent due to the $C_{3v}$ symmetry of the

system. All four $e$ MOs contain appropriate bonding combinations of the $Np$ and $1s$ orbitals of the three neighboring hydrogens. The $e_x$ and $e_y$ pairs of MOs, like $(3a_1, 4a_1)$, may thus be considered as internally bonding in the two $NH_3$ units. As in the previous two $a_1$ pairs, the antisymmetric combination of the left and right-hand space, with a nodal surface passing through the NN midpoint, is the higher energy MO of each pair $(2e)$.

The last four MOs of $(O_2H_5)^+$ are of $b_2$ and $b_1$ symmetry. The $b_2$ pair are quite similar to the $e$ MOs of $(N_2H_7)^+$ and are likewise considered as internal OH bonding orbitals. The $b_1$ pair are simple symmetric and antisymmetric combinations of the "$pi$" or $2p_x$ atomic orbitals of the two oxygen atoms and contain no contributions from any other orbitals. Along with the $(5a_1, 6a_1)$ pair, the $b_1$ set may be described as containing oxygen lone pair character.

The MOs depicted in Fig. 3 are those of the midpoint $(X—H—X)$ configuration. As described below, the MOs of the endpoint $(X–H---X)$ geometry are similar in appearance although the left-right symmetry of each MO in Fig. 3 is absent.

### A. $a_1$ orbitals

More accurate (less schematic) representations of each MO may be obtained by illustrating the electron density associated with the MO as a contour map. The density of the $5a_1$ MO for the midpoint $(N—H—N)$ structure of $(N_2H_7)^+$ is presented in Fig. 4(a). It is emphasized that this is *not* a difference map. The density (equal to twice the square of the absolute magnitude of the wave function) is everywhere positive. The position of the central proton is indicated by the dot at the midpoint of the N—N axis. The figure illustrates the covalent H-bonding character of the $5a_1$ orbital via the charge accumulation along the N—H—N axis. The $5a_1$
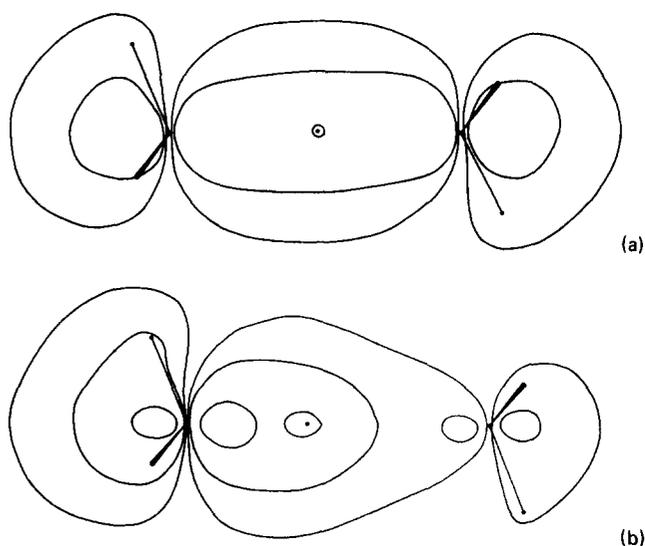


FIG. 4. Contour plot of electron density in the $5a_1$ MO of $(N_2H_7)^+$ in the (a) midpoint N–H–N and (b) equilibrium N–H---N geometries. The dot near the center represents the central proton. Densities associated with the contours are 0.2, 0.02, and 0.002 $e/a.u.^3$
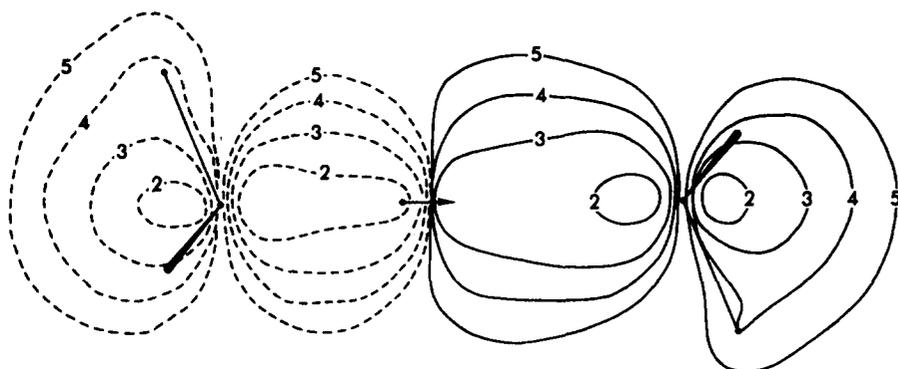
FIG. 5. Density difference map for the $5a_1$ MO of $(N_2H_7)^+$. Contours represent the difference in density between the midpoint (N–H–N) [Fig. 4(a)] and equilibrium N–H---N [Fig. 4(b)] geometries. Conventions for contour labels are as in Fig. 2.

MO is illustrated for the equilibrium (N–H---N) geometry in Fig. 4(b). The asymmetry introduced by the shifting of the central proton towards the left of the N—N midpoint has resulted in a skewing of the density to the left; i.e., more density is located in the vicinity of the proton-donating than accepting molecule.

Subtraction of the density of the equilibrium structure (Fig. 4(b)) from that of the midpoint Fig. (4a) yields the density difference map of Fig. 5. This map represents the charge rearrangements associated with the $5a_1$ MO that accompany half proton transfer. The pattern of broken and solid contours demonstrates a substantial shift of charge from left to right. This feature is a direct result of the skewing of density to the left in Fig. 4(b).

A similar analysis of the $6a_1$ MO shows a symmetric density in the (N—H—N) configuration and a skewing of the density to the *right* in the (N–H---N) geometry. The electron density rearrangement associated with the $6a_1$ MO, illustrated in Fig. 6, therefore contains a net shift of electrons from right to left; i.e., in the opposite direction than for $5a_1$. The aforementioned character-istics are common to all pairs of MOs: In the (X–H---X) geometry, the density is skewed towards the proton-donating molecule in the orbital of lower energy and to-wards the proton-accepting molecule in the higher en-ergy MO. Subtraction of the (X–H---X) density from the symmetric (X—H—X) function therefore leads to a charge shift from left to right in the lower energy MO and in the opposite direction for the partner orbital of the pair. Combination of these two gross effects leads to large-scale cancellation and reveals more subtle and informative features of electronic rearrangements. The most interesting information thus arises from study

of charge shifts occurring within each *pair* of MOs.

Addition of the density redistributions contained in Figs. 5 and 6 yields the charge shifts associated with the $(5a_1, 6a_1)$ pair of MOs of $(N_2H_7)^+$, shown in Fig. 7(a). The accompanying Fig. 7(b) illustrates corresponding changes in the $(5a_1, 6a_1)$ pair for $(O_2H_5)^+$. As was noted above for the total electron density (Fig. 2), we again observe strong similarities between the $(N_2H_7)^+$ and $(O_2H_5)^+$ systems. The patterns of $(5a_1, 6a_1)$ density changes about the central proton are nearly identical in either system to those observed for the total density of all ten occupied MOs. That is, the contours near the arrow are quite similar in Figs. 2 and 7. The excellent description in Fig. 7 of the shift in total density along with the motion of the central proton is not surprising since it is the $5a_1$ MO to which the $1s$ orbital of this H makes its major contribution.

A loss of electron density in the lone pair region of each proton-accepting atom is clearly indicated by the dashed contours to the left of the right hand X in Fig. 6. An analogous increase is observed in the lone pair regions to the right of each left hand X. We note that the changes in the lone pair regions are greater for $(O_2H_5)^+$ than for $(N_2H_7)^+$. For example, the smallest-labeled solid contour to the right of the proton-donating O is "3" as compared to a lowest value of "4" for the left hand N. Comparison of the areas enclosed by each broken contour to the left of the proton-accepting atoms leads to a similar conclusion for the right hand mole-cules.

The density changes in the lone pair regions associated with the $(5a_1, 6a_1)$ pair may be seen to be substantially greater than the corresponding changes in the total den-
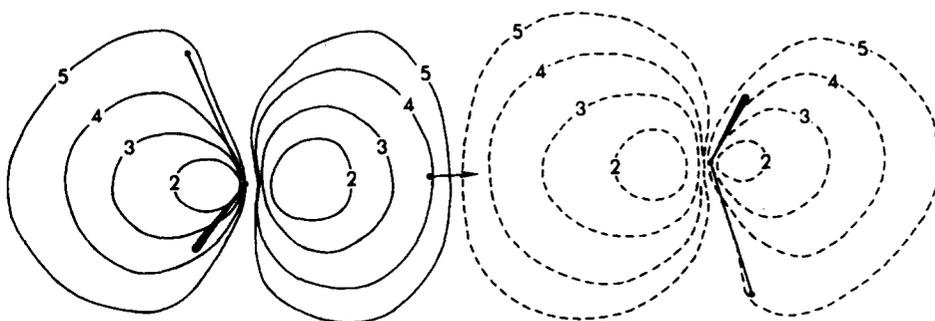


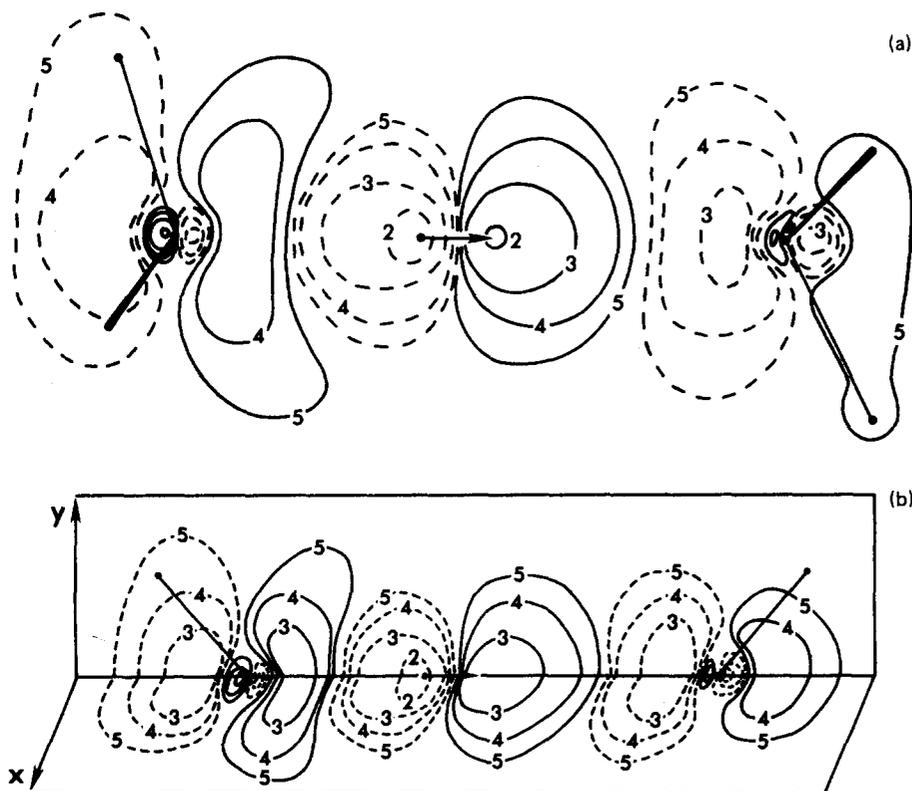FIG. 6. $6a_1$ density difference map of $(N_2H_7)^+$.

(a)

FIG. 7. Difference in density associated with the $(5a_1, 6a_1)$ pair of MOs in (a) $(N_2H_7)^+$ and (b) $(O_2H_5)^+$. Contour labels are defined in the caption to Fig. 2.

(b)

sity (Fig. 2). In fact, Fig. 2(a) shows a slight *loss* of total electron density in the lone pair region of the proton-donating N as compared to a sizable increase in Fig. 7(a).

A final feature of Fig. 7 is the internal shift of density occurring within each $XH_n$ molecule. The patterns of broken and solid contours clearly identify a shift from left to right across the X nucleus of each molecule. In addition, the maps indicate that these shifts are of greater magnitude for the $(O_2H_5)^+$ system than for $(N_2H_7)^+$. The contours about each right hand molecule

suggest that only a fraction of the charge lost on its left side is translocated across the X nucleus to the right, indicating a net transfer of the remaining density across the H-bond to the other molecule.

This charge transfer is indeed verified by Tables I and II which contain changes in Mulliken populations[20] resulting from the half proton transfer. The a superscript signifies the proton-donating molecule on the left and the accepting molecule is identified by the b superscript. Positive and negative entries, respectively, denote gains and losses of electron density (in millielectrons). We consider here the first column of each table which is pertinent to the $(5a_1, 6a_1)$ pair of MOs. The value of $-101$ me listed in Table I for the proton-accepting

TABLE I. Changes in Mulliken populations (millielectrons) resulting from half proton transfer in $(N_2H_7)^+$. Positive entries correspond to increases in population.

| | $(5a_1, 6a_1)$ | $(3a_1, 4a_1)$ | All $a_1$ | All $e$ | Total |
|---|---|---|---|---|---|
| **groups** | | | | | |
| $(NH_3)^a$ | 104 | 10 | 113 | 0 | 113 |
| $(NH_3)^b$ | $-101$ | $-5$ | $-106$ | 0 | $-106$ |
| **atoms** | | | | | |
| $H^c$ | $-2$ | $-5$ | $-7$ | 0 | $-7$ |
| $N^a$ | 144 | $-30$ | 113 | $-81$ | 32 |
| $H^a$ | $-13$ | 13 | 0 | 27 | 27 |
| $N^b$ | $-124$ | 30 | $-94$ | 89 | $-5$ |
| $H^b$ | 8 | $-12$ | $-4$ | $-30$ | $-34$ |
| **orbitals** | | | | | |
| $N^a$   $2s$ | 42 | $-42$ | 0 | 0 | 0 |
|     $2p_z$ | 101 | 12 | 113 | 0 | 113 |
| $N^b$   $2s$ | $-31$ | 42 | 11 | 0 | 11 |
|     $2p_z$ | $-93$ | $-12$ | $-105$ | 0 | $-105$ |

[a]Proton donor.      [c]Central proton.
[b]Proton acceptor.

TABLE II. Mulliken population changes in $(O_2H_5)^+$. Notations are the same as in Table I.

| | $(5a_1, 6a_1)$ | $(3a_1, 4a_1)$ | All $a_1$ | All $b$ | Total |
|---|---|---|---|---|---|
| **groups** | | | | | |
| $(OH_2)^a$ | 102 | 18 | 120 | 0 | 120 |
| $(OH_2)^b$ | $-86$ | $-6$ | $-91$ | 0 | $-91$ |
| **atoms** | | | | | |
| $H^c$ | $-16$ | $-13$ | $-29$ | 0 | $-29$ |
| $O^a$ | 117 | $-15$ | 102 | $-55$ | 48 |
| $H^a$ | $-7$ | 16 | 9 | 27 | 36 |
| $O^b$ | $-82$ | 16 | $-66$ | 54 | $-12$ |
| $H^b$ | $-2$ | $-11$ | $-13$ | $-27$ | $-40$ |
| **orbitals** | | | | | |
| $O^a$   $2s$ | 56 | $-33$ | 23 | 0 | 23 |
|     $2p_z$ | 60 | 19 | 79 | 0 | 79 |
| $O^b$   $2s$ | $-45$ | 31 | $-15$ | 0 | $-15$ |
|     $2p_z$ | $-37$ | $-14$ | $-51$ | 0 | $-51$ |

(a)
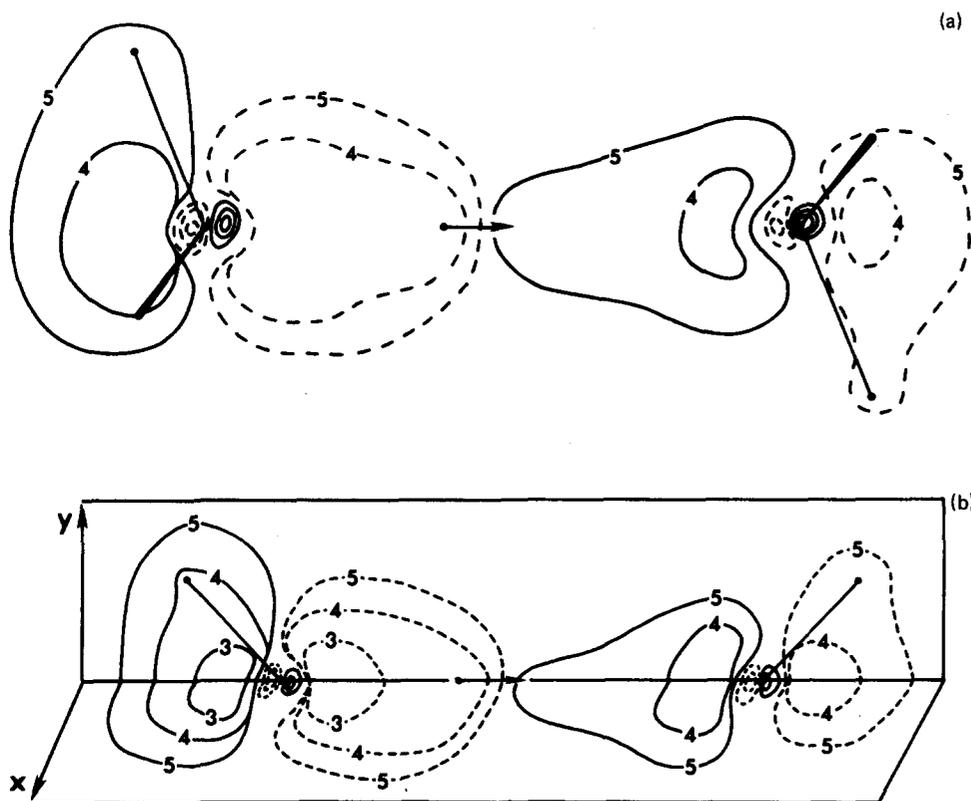


FIG. 8. Density difference maps for the $(3a_1, 4a_1)$ pair of (a) $(N_2H_7)^*$; (b) $(O_2H_5)^*$.

(b)

$(NH_3)^b$ molecule provides further demonstration of net density loss from this group within the $(5a_1, 6a_1)$ pair. Approximately the same amount of charge (104 me) is added to the other $NH_3$ molecule. A smaller amount of density (86 me) is withdrawn from the $(OH_2)^b$ molecule while 102 me accumulates on $(OH_2)^a$. The remaining charge (16 me) is removed from the central proton $H^c$ upon reaching the midpoint of the H-bond.

In order to provide more detailed information, the molecular charges may be further partitioned into contributions from individual atoms. The data in Tables I and II suggest that the great bulk of charge transfer within the $(5a_1, 6a_1)$ pair involves the X atoms with the noncentral hydrogens $H^a$ and $H^b$ playing only a minor role. Figure 7 confirms this conclusion as only small density changes are signified by the contours proximate to these hydrogens. Comparison of Tables I and II indicates that the net density changes undergone by the N atoms are somewhat larger than oxygen and secondly, that the increases experienced by the left hand X atoms are somewhat greater than decreases of the proton-accepting $X^b$ atoms.

The last several rows of Tables I and II provide information about the relative involvement of the $s$ and $p$ orbitals of the X atoms in the density changes undergone by each atom as a whole. The $2p_z$ orbitals are oriented along the internuclear X—X axis, while the perpendicular $2p_x$ and $2p_y$ orbitals are not of $a_1$ symmetry and are consequently unaffected by changes occurring within the $a_1$ MOs. We find that, whereas the $2s$ and $2p_z$ orbitals of the O atoms share approximately equally in the net atomic charge changes, the $2p_z$ orbitals of N undergo much greater changes than do the $2s$ orbitals.

Figure 8 depicts the charge shifts associated with the $(3a_1, 4a_1)$ pair of MOs. We note first the striking similarity between the contour patterns for the $(N_2H_7)^*$ Fig. 8(a) and $(O_2H_5)^*$ 8(b) systems. The principal feature of Fig. 8 is the shift of density from right to left across each X nucleus. This shift is in the opposite direction to the charge motion characterizing the $(5a_1, 6a_1)$ pair. Along the same vein, Tables I and II demonstrate also the opposite trends in the two pairs; the changes in most atomic charges for the $(3a_1, 4a_1)$ pair are of opposite sign to those of $(5a_1, 6a_1)$. As noted for $(5a_1, 6a_1)$ the X atoms undergo greater density changes within the $(3a_1, 4a_1)$ pair than do the peripheral H atoms, although these changes are considerably reduced in magnitude relative to $(5a_1, 6a_1)$.

Another conclusion from Tables I and II is that only a very small amount of charge is transferred from one molecule to the other via the $(3a_1, 4a_1)$ pair. This fact is in accord with the contour patterns of Fig. 8. That is, broken contours with a given label near each X nucleus are balanced by a similar solid contour to the left of the nucleus.

The population changes of the $s$ and $p$ orbitals of the X atoms in the $(3a_1, 4a_1)$ pair show several interesting features. For each atom, the $2s$ and $2p_z$ orbitals undergo changes of opposite sign. The $s$ orbital of each proton-donating atom loses density while an increase of somewhat smaller magnitude is noted in the $p$ orbital. This combination leads to the overall charge depletion observed in the proton-donating atom; exactly reverse trends occur within the accepting atom. The greater involvement of $s$ than $p$ orbitals is quite reasonable here since the latter orbitals make only minor contributions
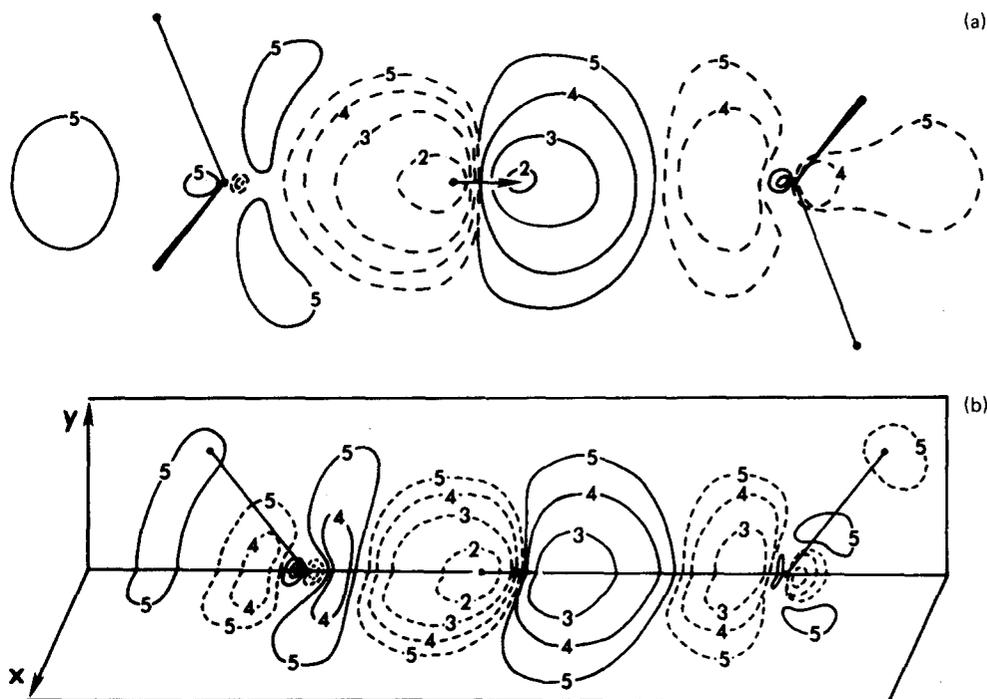
(a)

(b)

FIG. 9. Density rearrangements contained in the $(3a_1, 4a_1, 5a_1, 6a_1)$ MOs of (a) $(N_2H_7)^+$, (b) $(O_2H_5)^+$.

to the $3a_1$ and $4a_1$ MOs.

The density shifts in opposite directions of the $(3a_1, 4a_1)$ and $(5a_1, 6a_1)$ pairs result in a great deal of cancellation when the two density difference maps are combined. What remains as the most prominent feature of Fig. 9, representing the density rearrangements associated with all the $a_1$ MOs, are the electron density shifts along with the central proton. The density changes in the lone pair regions associated with $(5a_1, 6a_1)$ have been substantially reduced in magnitude by addition of the $(3a_1, 4a_1)$ effects. Comparison of Figs. 9(a) and 9(b) indicate greater $a_1$ density changes in the lone pairs of O than of N. Secondly, for both $(N_2H_7)^+$ and $(O_2H_5)^+$, the density loss in the right-hand lone pair is greater than the corresponding increase in the lone pair of the proton-donating atom. In fact, the small charge buildup for $N^a$ is centered not along the N—N axis as one might expect but rather in two symmetric locations above and below the axis.

Figure 9 illustrates that a primary rearrangement effect of the $a_1$ orbitals is a net transfer of charge from the proton-accepting molecule on the right to the donating molecule. The charge depletion from the right-hand molecule originates not only in the lone pair of X, but also in a region directly behind it. Analogously, charge accumulation is observed both in front of and behind the left-hand X atom.

The absence of strong contours near the noncentral hydrogens indicates that these atoms are little involved in $a_1$ rearrangements. Indeed, this conclusion is affirmed by the third column of Tables I and II which point to the X atoms as the source and sink of $a_1$ electronic redistributions. The nitrogen atoms undergo greater changes in atomic charge than do the O atoms. This observation is in interesting contrast to the aforementioned fact that rearrangements in the lone pair regions

of N are *smaller* in magnitude than for O. We may conclude, therefore, that the density changes occurring *behind* the X atoms are greater for $(N_2H_7)^+$ than for $(O_2H_5)^+$. In other words, the $a_1$ density changes of the O atoms are more heavily concentrated on the "inside" of the H-bond (i. e., towards the central proton) than is true for N.

Some justification of this trend may be provided by the $s$ and $p$ orbital population changes. Reinforcement of $(3a_1, 4a_1)$ and $(5a_1, 6a_1)$ changes of $p_z$ orbital populations result in much larger $a_1$ changes within this atomic orbital than for $2s$ where some cancellation between the two MO pairs is noted. The net result is that the $a_1$ changes in N atomic charge are due almost exclusively to $p_z$ while for O the change is more evenly distributed between $2p_z$ and $2s$. It must next be remembered that the density of the $p_z$ orbital is equally distributed between the $+z$ and $-z$ directions; i. e., inside and outside of the H-bond. Any biasing of density towards the inside requires hybridization of the orbital via combination with $2s$. The oxygen atoms, where the $2s$ shares in the atomic density changes to some extent, are thus better able than N to focus their density changes towards the inside of the H bond.

One may also describe the density rearrangements in Fig. 9 in terms of the contributions of the two pairs of MOs. In the lone pair regions of the X atoms (toward the H-bond center), the effects of the $(5a_1, 6a_1)$ pair are dominant, although attenuated somewhat by $(3a_1, 4a_1)$. The latter pair, primarily of XH bonding character, dominate the density changes on the opposite side (i. e., outside) of the X—X axis.

## B. Non-$a_1$ orbitals

We now turn to the remaining four occupied MOs of each system. The density rearrangements associated
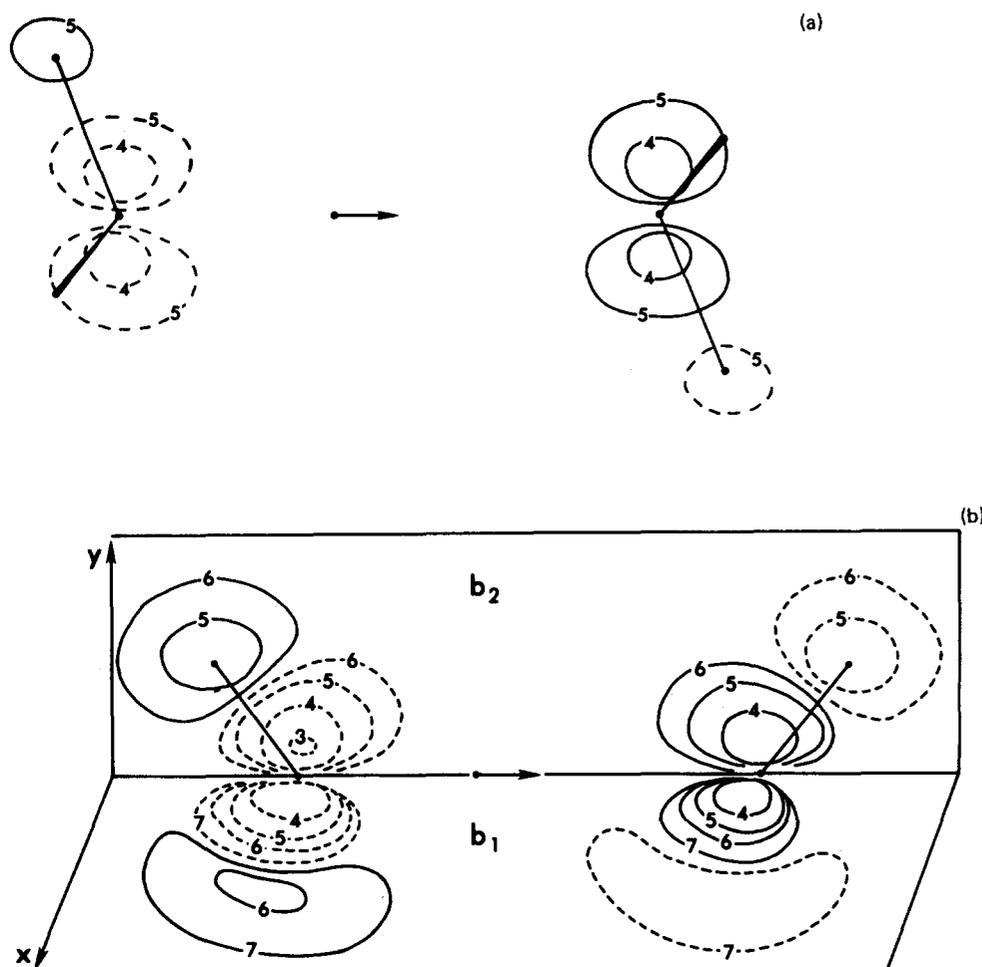
(a)

(b)

FIG. 10 (a) Density changes in the $(1e_x, 2e_x)$ pair of $(N_2H_7)^+$; (b) difference maps for the $(1b_1, 2b_1)$ and $(1b_2, 2b_2)$ pairs of $(O_2H_5)^+$. Contour labels as high as 7 are provided for $(O_2H_5)^+$.

with the $(1e_x, 2e_x)$ pair lying in the $xz$ plane of $(N_2H_7)^+$ are illustrated in Fig. 10(a). Shifts occurring within the $(1e_y, 2e_y)$ pair are not presented since the latter pair is equivalent to $e_x$ as a result of the $C_{3v}$ symmetry. Density shifts associated with the inequivalent $b_1$ and $b_2$ pairs of $(O_2H_5)^+$, lying in the $xz$ and $yz$ planes, respectively, are illustrated in Fig. 10(b). In order to point out certain important features, additional contours that encompass density differences of as little as $10^{-7/2}$ e/au$^3$ (the "7" contours) have been included in this figure.

As described previously, the $b_2$ orbitals of $(O_2H_5)^+$ are quite similar to the $e$ MOs of $(N_2H_7)^+$. The principal charge rearrangement occurring within these pairs, as may be seen in Fig. 10, is internal polarization of the XH bonds. Density is shifted within the proton-accepting molecule from peripheral hydrogen atoms to the appropriate $p$ orbital of X; the direction of polarization is reversed in the left hand molecule. This pattern is confirmed by the atomic charges in the fourth column of Tables I and II. The group charges indicate as well that no density is transferred between molecules via the non-$a_1$ orbitals; i.e., all charge rearrangements are internal. Thus, the sum of charge differences of the $n$ H atoms of a given XH$_n$ molecule are precisely equal and opposite to the change of the X atom. In addition, we note a surprising degree of uniformity in charge differences: all noncentral H atoms experience a gain or loss

of $\sim 27$ me. The result of this fact is that the N atoms, bonded to three hydrogens, show larger atomic charge differences than do the oxygens which are bonded to only two H atoms.

With regard to the individual atomic orbitals, the changes recorded for the N atoms in the fourth column of Table I are split equally between the equivalent $p_x$ and $p_y$ orbitals. The oxygen atomic charge differences are due solely to the $p_y$ orbitals. The $p_x$ orbitals remain doubly occupied as the proton is transferred. The $s$ and $p_z$ orbitals are of $a_1$ symmetry and are hence, excluded from interacting with the non-$a_1$ MOs.

The density shifts occurring within the $b_1$ orbitals of $(O_2H_5)^+$ are particularly enlightening. These MOs are comprised exclusively of $p_x$ atomic orbitals of the O atoms and are consequently orthogonal to the H orbitals centered in the $yz$ plane. Even though the H atoms may not participate in the $b_1$ charge rearrangements, the contour patterns are not entirely unlike the $b_2$ shifts where hydrogens play a major role. Both $b_1$ and $b_2$ patterns indicate a flow of electrons inward toward the proton-accepting O$^b$ nucleus. In the $b_2$ pair, the source of this density is the noncentral H atoms. With no such source available, the $b_1$ pair attracts electrons instead from a much larger and more diffuse region of space encompassed by the broken "7" contour. This "x-polarization" of the $p_x$ orbital occurs via an increase in the

coefficient of the inner $2p_x$ function at the expense of the outer, more diffuse $2p_x$ of the split valence-shell. The reverse is true on the left-hand O atom where the diffuse outer $2p_x$ function is used as an electron sink. It should be noted that the charge rearrangements found here in the $xz$ plane of $(O_2H_5)^+$ would not be possible with use of a smaller minimal basis set containing only one $p_x$ orbital for each O atom.[26]

## V. ORIGINS OF DENSITY SHIFTS

Many of the charge redistributions described above may be attributed to simple electrostatic factors. The approach of a proton with its positive charge is expected to "pull" electrons towards it. The symmetry of the non-$a_1$ orbitals (viz., $e$, $b_1$, $b_2$) facilitates electron motion in a direction perpendicular or "transverse" to the H-bond axis. Hence, as the proton approaches the right-hand molecule, density is attracted towards this axis; viz., towards the X atom. For the $e$ MOs of $(N_2H_7)^+$ and the $b_2$ pair of $(O_2H_5)^+$ the density is drawn away from the peripheral H atoms and we characterize this phenomenon as internal polarization of the XH bonds. The $b_1$ pair of $(O_2H_5)^+$, on the other hand, is forbidden by symmetry from interacting with the hydrogens and consequently the electronic rearrangement towards the O atom is of much smaller magnitude. Motion of the central proton away from the left-hand molecule results in a reverse charge shift away from the X—X axis.

The symmetry of the $(3a_1, 4a_1)$ pair allows "longitudinal" density shifts parallel to the X—X axis. As the proton moves from left to right, density is drawn towards it in the right-hand molecule. The additional density in the lone pair region to the left of the X nucleus accumulates at the expense of the XH bonds to the right of the X. These redistributions may be described as internal XH → lone pair shifts. Motion of the proton away from the left-hand molecule decreases the pull on the right side of the molecule, resulting in a lone pair → XH polarization. In either case, the electronic motion is right to left (see Fig. 8).

The redistributions within the $(5a_1, 6a_1)$ pair, however, are not influenced solely by electrostatic considerations since these MOs also include covalent interactions with the transferring proton. Effects observed within this MO pair include a thinning out of the proton-accepting lone pair as these electrons "reach out" to meet the approaching proton and an analogous density increase in the lone pair of the proton-donating atom. The $(5a_1, 6a_1)$ pair serves also as the medium by which charge is transferred across the H bond from one molecule to the other. Density shifts occurring within $(5a_1, 6a_1)$, like those of $(3a_1, 4a_1)$, are longitudinal rearrangements.

Addition of the electronic redistributions in Fig. 10 to those associated with the $a_1$ orbitals (Fig. 9) leads finally to the total density difference maps of Fig. 2. We are now in a position to analyze the total density shifts and to assign each of the various regions of Fig. 2 to the appropriate MO from which it arises. The density shifts about the central proton are attributed to the $(5a_1, 6a_1)$ pair of MOs and, in fact, primarily to $5a_1$ which con-

tains the largest contribution from the $1s$ orbital of the central hydrogen. The electronic rearrangements around the peripheral hydrogens arise chiefly from polarizations of the XH bonds which originate in the MOs of non-$a_1$ ($e$ or $b_2$) symmetry. The effects of the $a_1$ MOs upon these hydrogens are rather small due to two factors. First, the charge rearrangements associated with these MOs are concentrated along the H-bond axis. Secondly, the effects of the $(5a_1, 6a_1)$ and $(3a_1, 4a_1)$ pairs upon these H atoms tend to cancel one another. The slightly greater total density changes about the peripheral hydrogens of $(O_2H_5)^+$ than of $(N_2H_7)^+$ are due to a small degree of reinforcement of the $b_2$ pair by the $a_1$ MOs in the former system.

The decrease in total density in the lone pair region to the left of the proton-accepting atom may be traced back unambiguously to the $(5a_1, 6a_1)$ pair; more specifically to the $6a_1$ MO. This charge depletion is tempered somewhat by the $(3a_1, 4a_1)$ pair and the extent of the region is compressed toward the H-bond axis by density increases of the $p_x$ and $p_y$ atomic orbitals associated with the non-$a_1$ MOs. The analogous density accumulation in the lone pair of the proton-accepting atom is much smaller in magnitude and is in fact absent in $(N_2H_7)^+$. The smallness of the increase is due primarily to effective cancellation in this region between the opposite trends of the $(5a_1, 6a_1)$ and $(3a_1, 4a_1)$ pairs. The increase is further eroded by the charge depletions associated with the non-$a_1$ orbitals. The "outward" polarization of the $p_x$ orbital of the proton-donating oxygen accounts for the fact that the lone pair increase of this atom lies largely in the $xz$ plane.

The regions of density loss lying along the H-bond axis and directly behind the proton-accepting atom (i.e., away from the central proton) are due exclusively to the $a_1$ MOs. In particular, the density is drawn out of the XH bonding region and pulled across the X nucleus into the X lone pair by the $(3a_1, 4a_1)$ pair. The shape of this region and the magnitude of density change are modified by a lesser increase due to the $(5a_1, 6a_1)$ pair. Similar arguments apply to the charge gain behind the proton-donating atom on the left.

The lobes of density increase surrounding the proton-accepting atom have their origin in the HX bond polarizations of the non-$a_1$ MOs. For $(O_2H_5)^+$, the lobes in the $xz$ plane represent smaller increases than in the $yz$ plane since there are no H atoms in the former plane. Thus, this density must be drawn in toward the O nucleus at the expense of a broad region farther out in the $xz$ plane. The nearly circular lobes noted in Fig. 10 are "pushed" out away from the center of the H bond by combination with the $a_1$ density decreases in the lone pair region. Fusing of these lobes with a small region of $a_1$ charge increase directly to the left of the nucleus along the H-bond axis produces the final shape observed in Fig. 2. The dashed lobes on the left-hand atom owe their shape to analogous factors. We note in addition that the dashed contours of these lobes in Fig. 10(b) coalesce with similar contours behind $O^a$ in Fig. 9(b) to form a continuous region of density depletion that completely surrounds the left hand O atom in Fig. 2(b).

As a last point, it is also possible to pinpoint the source of the charge being transferred along the H bond from the proton-accepting to the donating molecule. As may be seen in Tables I and II all of the charge transfer takes place via orbitals of $a_1$ symmetry. In addition, the $(5a_1, 6a_1)$ pair is responsible for most of this transfer with only a minor ($\sim 8\%$) additive contribution from $(3a_1, 4a_1)$. Further analysis reveals that the X atoms are the primary source and sink of the charge transfer with the peripheral hydrogens playing only a minor (and opposite) role. Finally, the atomic orbital populations indicate a major difference between the N and O atoms in that the $2s$ and $2p_z$ orbitals of O are approximately equally involved in the charge transfer, whereas the $2p_z$ orbital of N plays a much more significant role than $2s$.

## VI. CONCLUSIONS

Partitioning of rearrangements of the total electron density resulting from proton transfer into separate contributions from the occupied molecular orbitals provides a great deal of insight into the various factors involved. Charge migrations transverse to the H-bond axis are responsible for polarizations of the XH bonds and the associated density changes about the noncentral H atoms. Internal density shifts between lone pairs and XH bonds of each $XH_n$ molecule result from longitudinal polarizations of the electronic distribution. The above features are readily explained in terms of attraction between the molecular electron cloud and the positively charged proton being transferred. The thinning out of density in the lone pair of the proton-accepting atom is due to covalent effects as the electrons extend themselves towards the approaching proton. Only very small density accumulations are observed in the proton-donating lone pair due to a cancellation of opposing effects. The covalent buildup is counteracted by electrostatic forces that pull electrons out of the lone pair and into the XH bonds. The charge transferred from the proton-accepting to the donating molecule originates in the $2s$ and $2p_z$ atomic orbitals of the X atoms; the "covalent" MOs are the vehicle of this transfer.

In addition, it is possible to explain characteristic and apparently complex differences between the nitrogen and oxygen-containing systems in terms of simple properties such as relative involvement of $s$ and $p$ atomic orbitals and number of bonded H atoms.

## ACKNOWLEDGMENTS

[1] S. Scheiner, J. Am. Chem. Soc. 103, 315 (1981).
[2] S. Scheiner, Ann. N.Y. Acad. Sci. 367, 493 (1981).
[3] S. Scheiner and L. B. Harding, J. Am. Chem. Soc. 103, 2169 (1981).
[4] S. Scheiner and L. B. Harding, Chem. Phys. Lett. 79, 39 (1981).
[5] S. Scheiner, J. Phys. Chem. (to be published).
[6] S. Scheiner, Int. J. Quantum Chem. QBS8, 1981 (in press).
[7] W. Meyer, W. Jakubetz, and P. Schuster, Chem. Phys. Lett. 21, 97 (1973).
[8] W. P. Kraemer and G. H. F. Diercksen, Chem. Phys. Lett. 5, 463 (1970).
[9] R. Janoschek, E. G. Weidemann, H. Pfeiffer, and G. Zundel, J. Am. Chem. Soc. 94, 2387 (1972).
[10] P. A. Kollman and L. C. Allen, J. Am. Chem. Soc. 92, 6101 (1970).
[11] P. Merlet, S. D. Peyerimhoff, and R. J. Buenker, J. Am. Chem. Soc. 94, 8301 (1972).
[12] J.-J. Delpuech, G. Serratrice, A. Strich, and A. Veillard, Mol. Phys. 29, 849 (1975).
[13] S. Ikuta, Chem. Phys. Lett. 56, 490 (1978).
[14] B. O. Roos, W. P. Kraemer, and G. H. F. Diercksen, Theor. Chim. Acta 42, 77 (1976).
[15] A. Størgard, A. Strich, J. Almlöf, and B. Roos, Chem. Phys. 8, 405 (1975).
[16] M. D. Newton, J. Chem. Phys. 67, 5535 (1978).
[17] M. D. Newton and S. Ehrenson, J. Am. Chem. Soc. 93, 4971 (1971).
[18] W. J. Hehre, W. A. Lathan, R. Ditchfield, M. D. Newton, and J. A. Pople, QCPE, GAUSSIAN-70, Program No. 236 (1974).
[19] R. Ditchfield, W. J. Hehre, and J. A. Pople, J. Chem. Phys. 54, 724 (1971).
[20] R. S. Mulliken, J. Chem. Phys. 23, 1833 (1955).
[21] P. J. Desmeules and L. C. Allen, J. Chem. Phys. 72, 4731 (1980).
[22] G. H. F. Diercksen, Theor. Chim. Acta 21, 335 (1971).
[23] H. Umeyama and K. Morokuma, J. Am. Chem. Soc. 98, 7208 (1976).
[24] M. Dreyfus and A. Pullman, Theor. Chim. Acta 19, 20 (1970).
[25] P. A. Kollman and L. C. Allen, J. Chem. Phys. 52, 5085 (1970).
[26] On the other hand, further enlargement of the basis set via inclusion of polarization functions (Ref. 3) does not produce any additional qualitative changes in the 4-31G results described herein.